EXECUTIVE SUMMARY OF THE THESIS

Verification of two Operational Modal Analysis tools on Simulated and Full-Scale OWTs

LAUREA MAGISTRALE IN MECHANICAL ENGINEERING - INGEGNERIA MECCANICA

Author: BRUNO RODRIGUES FARIA

Advisor: PROF. ALBERTO ZASSO

Co-advisor: ALESSANDRO FONTANELLA

Academic year: 2021-2022

1. Introduction

Offshore Wind Turbines (OWTs) represent a great technological solution toward the green energy grid transition. This thesis work aims to further allow the extraction of meaningful data from operating wind turbines and the analysis of relevant tower modal parameters.

Operational Modal Analysis (OMA) tools have been widely used in civil engineering applications since they are output-only techniques and do not depend on artificially loading the structure as in many classic modal analysis. However, there is still a research gap on their limitations and capabilities when applied to OWTs. Long recording times, necessary for the identification of low frequency modes, on offshore installations, is linked with a compromise to the stationary nature of the excitation, as meteorological conditions are often changing. The robustness of the OMA techniques to the zero-mean loading assumption, explained in Sec.2, was pursued.

Two different OMA methods are sought to be validated: a single accelerometer technique (OMA Sing) [3] as a partially automated solution, presenting a classical peak-picking routine and an optimized version, described in Sec.2.1;

and a Covariance driven Stochastic Subspace Identification technique (OMA SSI-COV) [2] as a fully automated method with a more complex identification and multiple accelerometers, described in Sec.2.2. The OMA techniques were applied on both simulated, FAST Av04 model, and full-scale, Av07 measurements, data. The motivation leading such methodology is explained in Sec.3.

In parallel to that, many wind simulation standards do not distinguish between recommended total damping values for tower orthogonal direction modes. Such research gap is important to be studied once different levels of damping could play a major role in the OWT controller strategy and overall fatigue life. The along wind and cross wind closely spaced tower modes and their distinct modal damping ratios [4] were the focus of the OMA tools' identification. The goal was to examine whether there is a significant damping ratios' difference between the considered OWT's tower modes and, in the meanwhile, verify the OMA tools' performance for highly and lightly damped vibration responses.

2.   OMA Techniques

In Sec.2.1 and in Sec.2.2, the OMA Sing and the OMA SSI-COV have their routines respectively commented, highlighting advantages and drawbacks of each.

Before that, the white noise Gaussian derivation will be briefly commented below to explain the OMA tools' strongest assumption [1].

Starting from the consideration of a linear system characterized by the impulse response function, it is possible to relate

$$h(t) \leftrightarrow H(s) \tag{1}$$

where $H(s)$ is the Laplace Transform and it is usually seem as the associated Fourier transform $H(i\omega)$. Such a function can be used to represent the energy of the system $g(t)$ in the frequency domain as the time function

$$g(t) \leftrightarrow |H(i\omega)|^2 = H(i\omega)H^*(i\omega) \tag{2}$$

using the time reversal and the convolution property

$$g(t) = h(-t) \circledast h(t) \tag{3}$$

Conveniently, the correlation function of a system excited by a white noise with zero mean is as shown in Eq. 4. Several mathematical steps that support the equation below has been omitted and can be found in [1].

$$R_y(\tau) = 2\pi \frac{\sigma_x^2}{2B} h(-\tau) \circledast h(\tau) \tag{4}$$

where $2\pi \frac{\sigma_x^2}{2B}$ is a constant.

In conclusion, it can be noted that the correlation of the response in case of white noise excitation, Eq. 4, is proportional to the deterministic correlation function given by Eq. 3. In other words, it is proportional to the system energy or to the *Impulse Response Functions* (IRF), which leads to the identification of main modal parameters.

2.1.   OMA Sing

One of the simplest OMA methodologies to estimate modal parameters is based on the so-called peak-picking (PP) routine. The selection of eigen frequencies is done by identifying the peaks corresponding to the resonant frequencies from the power spectrum response of a line-like structure. There are two PP routines available

inside OMA Sing algorithm: one fully manual and a preferable automatized peak selection.

Even though OMA Sing has already been validated in civil engineering applications, it presents two major drawbacks. Firstly, it may require human intervention, being a biased tool in cases of noisy data, weakly-excited modes and relatively close eigenfrequencies, as it becomes highly subjective. Secondly, it is not able to calculate the mode shapes as only one acceleration point is considered.

2.2.   OMA SSI-COV

OMA SSI-COV is a rather more mathematically complex solution compared to OMA Sing, which uses multiple acceleration input. Its robustness to non ideal stationary load excited systems has already been observed in the study of vehicle-induced vibration of the Lysefjord Bridge. Further results' contributions on OWTs are sought in this thesis.

The six main routines that compose the OMA SSI-COV algorithm will be briefly commented on the items below

1. **Calculation of cross-correlation function**
   As explained by the white noise assumption derivation (check Eq.4), the cross-correlation function returns the IRF. The time lag for the covariance calculation was $8s$. The maximum time lag should range from two to six times the longest natural period chased. A down sampling was a applied by a factor of six without accuracy loss and less computational effort.

2. **Build of block Toeplitz matrix and SVD**
   Build a block-matrix with constant covariance matrices along parallels to the main diagonal (Toeplitz) and then derive its singular value decomposition, simplifying the block-matrix and illustrating interesting resulting matrices, as the *extended observability matrix* and the *reversed extended stochastic controllability*.

3. **Modal identification procedure**
   Extraction of the modal properties from the extended observability matrix of the system, such as fn, eigenfrequencies, ζ, damping ratios, and ϕ, mode shapes. Differ-

ent system's order (rows of the observability matrix or N_{max}) are set and shall be checked in the following step.

Algorithm 1 Stabilization Diagram Routine

1: initialize $N_{max} = 60$
2: **for** ii=N_{max}:-1:2 **do**
3:     jj= ii-1
4:     load modal parameters from two adjacent pole (ii,jj)
5:     $N(ii) = \text{size}(f_{ii})$ and $N(jj) = \text{size}(f_{jj})$
6:     **for** rr=1:N(ii) **do**
7:         **for** kk=1:N(jj) **do**
8:             calculate error of $f_{ii}(rr)$ and $f_{jj}(kk)$
9:             do the same for zeta and MAC
10:             compare them with respective thresholds δ_{freq}, δ_{zeta} and δ_{MAC}
11:             update $stab_{fn}$, $stab_{MAC}$ and $stab_{zeta}$

12:             **if** $stab_{fn} == 0$ **then**
13:                 stabStatus = 0
14:             **else if** $stab_{fn} == 1$ & $stab_{MAC} == 1$ & $stab_{zeta} == 1$ **then**
15:                 stabStatus = 1
16:             **else if** $stab_{fn} == 1$ & $stab_{MAC} == 0$ & $stab_{zeta} == 1$ **then**
17:                 stabStatus = 2
18:             **else if** $stab_{fn} == 1$ & $stab_{MAC} == 1$ & $stab_{zeta} == 0$ **then**
19:                 stabStatus = 3
20:             **else if** $stab_{fn} == 1$ & $stab_{MAC} == 0$ & $stab_{zeta} == 0$ **then**
21:                 stabStatus = 4
22:             **end if**
23:             fn = [fn, $f_{jj}(kk)$]
24:             zeta = [zeta, $zeta_{jj}(kk)$]
25:             MAC = [MAC, $MAC_{jj}(kk)$]
26:             Stability_Status = [Stability_Status, stabStatus]
27:         **end for**
28:     **end for**
29: **end for**
30: sort the found modal parameters vectors

---

4. **Stability checking procedure**
   The great number of poles and subsequent modes identified requires an automated stability checking procedure. For that, *Stabilization Diagrams* is used to distinguish structural poles from numerical poles or the so-called spurious poles, setting accuracy

tests in terms of percentage errors on frequency (δ_{freq}), damping ratio (δ_{zeta}) and MAC (δ_{MAC}), as shown in Alg.1.

5. **Selection of stable poles**
   Select only the stable modes, remove the negative damping modes (also considered unstable poles) and normalize the mode shapes for post-MAC building.

6. **Cluster Algorithm** Build MAC and construct agglomerative clusters from linkages, based on a criterion $eps_{cluster}$ of 0.2. The clustering routine plays a major role in the OMA SSI-COV automated functionality code by grouping, sorting and averaging modes previously found. It ignores clusters with less than ten elements (minor clusters).

3. OWT simulated and full-scale data

FAST model data and full-scale measurements of the 5MW OWTs from Alpha Ventus wind park are identified. The usage of FAST model provides an extra source of proof to the OMA performance as the stationarity of the load excitation is numerically guaranteed and there is no measurement noise included. On the other hand, full-scale data analysis should allow the understanding of OMA tools' performance whether the strong load assumptions are not completely respected.

3.1. FAST Model

The given thesis work based its modeling methodology on OC5 Phase III Par1[5]. A stepwise increasing complexity number of Load Cases (LC.x) is developed to co-validate codes. In this section, the missing validating results from the Av04 FAST model are pursued, before preparing the LCs to identify the tower modal parameters using the OMA tools.

The FAST model tower adjustment factors (TAF) were tuned for a better match with the reference SWE model's fore aft tower eigen frequency. The *FAStTunr(1)* and *SSStTunr(1)* parameters were set to **0.86**, achieving an error of **5.1%**. The fore aft (along wind) and side to side (cross wind) eigen frequencies, found by means of the Fast Fourier Transform (FFT) spectrum, were **0.353Hz** and **0.343Hz** respectively.

The following steady and turbulent wind simu-

lations were conducted
- **LC "1":** Rotor Speed as function of Wind Speed.
- **LC "2":** Tower Top Fore Aft Shear Force - Turbulent Mean Wind Speed of 16m/s.
- **LC "3":** Tower Top Fore Aft Displacement - Deterministic Wind Speeds of 6-7m/s.
- **LC "4":** Tower Top Fore Aft Displacement - Deterministic Wind Speeds of 17-18m/s.

The statistics function chosen to standardize the participants' performance was the non-dimensional root mean square error (NRMSE).

	FAST		**Participants Average**
	Biased	**Detrend**	
LC "1"	-	5.7%	not given
LC "2"	-	17.9%	14.3%
LC "3"	23.9%	13.9%	14.4%
LC "4"	35.8%	18.7%	12.6%

Table 1: FAST model performance (NRMSE) against other participants in OC5.

The Av04 FAST model was validated since it showed on average an NRMSE below 20% for the detrend results, which is considered a good match between model and reference. The biased results did not consider the steady state influence of the updated TAF.

3.2. RAVE Data - Wind and Acceleration

Meteorological, operational and dynamic data were accessed through the SCADA monitoring and the FINO substation. The month of November 2015 was chosen due to high availability and quality of measurements.

Unfortunately, due to the lack of long non-NaN acceleration recordings, tower instrumentation and reported maintenance's problems by employees, it was not possible to analyze Av04 full-scale. The Av07 showed to be the most well-instrumented OWT and the spatially closer turbine to Av04. Similar variable-speed pitch-to-feather controller settings, blade pitch and rotor speed, were found visualizing Av04 FAST model and Av07 SCADA operating data, which encourages a qualitative analysis of results.

3.2.1 Wind Seeds

Following OC5 report, wind conditions from below rated wind speed (8 ms^{-1}) and above rated wind speed (19 ms^{-1}) were selected, each with six seeds. In parallel, their stochastic properties (30-minute average and 20 Hz) were used as reference for the TurbSim grid generation to be utilized in the FAST's input. Two extra wind speeds' seeds (13 ms^{-1} and 23 ms^{-1}) were extracted for the sake of results' robustness in Sec.4.2.

3.2.2 Nacelle Accelerometer

The Nacelle accelerometers were available in four outputs. Due to poor documentation, a investigative campaign had to be pursed using OMA Sing to identify the modal parameters for above and below rated wind speed and validate the sensors direction. This thesis concluded that $M7\_B\_D56v\_x$ and $M7\_B\_D56v\_y$ detected cross wind and along wind nacelle motions, opposite to the RAVE documentation.

Data was available in a sampling frequency of $50Hz$ and the stochastic characteristics were calculated on 30-minute average time.

3.2.3 Tower Accelerometers

The Av07 tower is instrumented with five pairs of accelerometers in different height positions. At each height, the sensors signals were summed and averaged, removing the torsional component and reducing the measurement noise.

Besides that, the unsure sensors location and unreliable wind direction data requested the application of a novel solution. The principal component analysis (PCA) was applied to retrieve the linearly uncorrelated along wind and cross wind variables with respect to the wind excitation.

The tower accelerometers' sampling frequency and averaging time were the same from the nacelle accelerometers.

4. Evaluation of OMA tool's Identification

For the sake of robustness and quantitative comparison, before applying the OMA tools, a classical mean logarithmic decay (MLD) method was performed in specific Av04 FAST LCs. The MLD method can only be applied on the FAST

Av04 model due to the necessity of a free decay response.

4.1. MLD Reference Method

The stepwise FAST procedure to extract the reference modal parameters from the numerical model using MLD is shown in Fig.1.
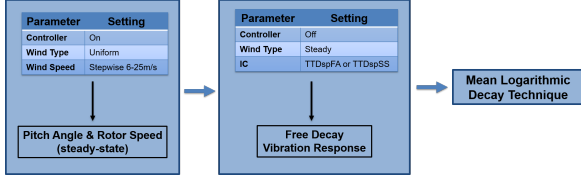

Figure 1: Logarithmic Decay Methodology Schematic by blocks.

Once the free decay vibration responses were available for each wind speed in along wind and cross wind tower direction, the local modal parameters were extracted as shown in Eq.5.

$$
\begin{cases}
f_{kk} = (\dfrac{1}{\Delta t_{kk}}), & (5a) \\[2mm]
\delta_{kk} = \ln(\dfrac{pks_{kk}}{pks_{kk+1}}), & (5b) \\[2mm]
h_{kk} = \dfrac{1}{\sqrt{1 + (\frac{2\pi}{\delta_{kk}})^2}}. & (5c)
\end{cases}
$$

where Δt_{kk} represents the time interval of two consecutive peaks, pks is the amplitude of the given peak, dt is the simulation time step and $kk = [1, 2, \cdots, n]$.

Afterward, the local modal parameters were averaged inside of a linear trend region and therefore n was manually defined for each decay vibration response, as derived in Eq.6.

$$
\begin{cases}
f_n = \dfrac{1}{n}(\sum_{kk=1}^{n} f_{kk})[Hz], & (6a) \\[3mm]
h = \dfrac{100}{n}(\sum_{kk=1}^{n} h_{kk})[\%]. & (6b)
\end{cases}
$$

Even though MLD was a highly manual method, it provided extra source of validation for the OMA tools' modal identification.

4.2. OC5 Load Cases

Following OC5 methodology, four wind speeds scenarios, each containing six winds seeds with equal wind stochastic properties, were analyzed

by the presented tools.

Two distinct modal damping ratios' orders of magnitude were observed for the orthogonal tower modes (along wind and cross wind) using MLD, OMA Sing and OMA SSI-COV.

In Fig.2(b) the cross wind tower motion of the Av04 FAST model was identified. The two OMA tools showed great accuracy on the eigen frequencies compared to MLD, with a maximum error of 2.7% and uncertainty of 1.1%. OMA SSI-COV had a slight performance advantage in terms of damping ratio extraction, better illustrating the aerodynamic contribution at higher wind speeds. On the other hand, the OMA SSI-COV identification of the along wind motion was rather delicate, as shown in Fig.2(a). Differently from OMA Sing, it presented large eigen frequency variability for the 23ms^{-1} seed, resulting in a non reliable and over predicted damping ratio for higher wind speeds. Such behavior will be further analyzed.

As for the FAST model, the full-scale Av07 eigen frequency identification of the cross wind tower motion were more accurate than for along wind. Figure 2(b) illustrate it. Cross wind damping is mostly composed by structural contribution.
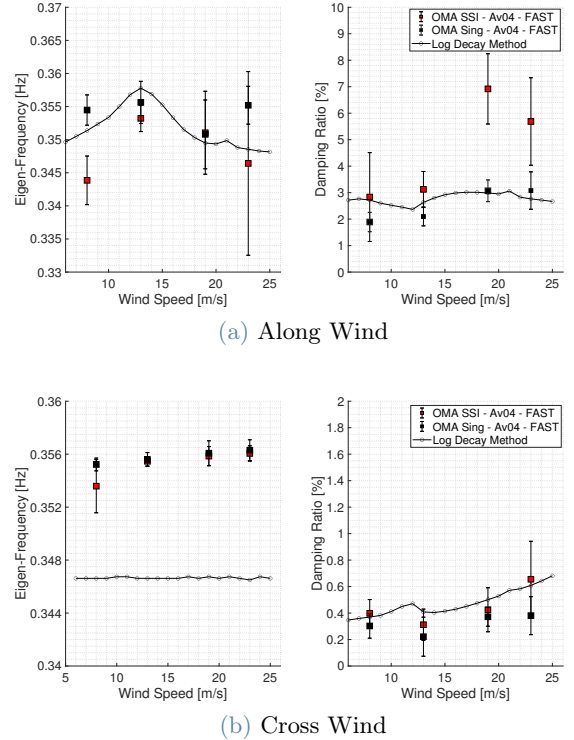

(a) Along Wind

(b) Cross Wind

Figure 2: FAST Av04 Error Bar Plot of OMA Sing and OMA-SSI Modal Parameters against MLD.
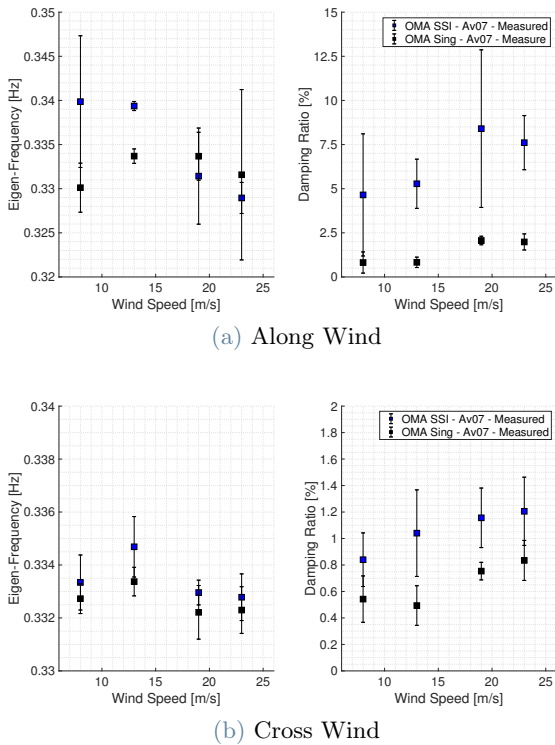
(a) Along Wind

(b) Cross Wind

Figure 3: Full-Scale Av07 Error Bar Plot of OMA Sing OMA SSI-COV Modal Parameters.

The damping ratio of OMA SSI-COV averages around 1%, which is a standard on OWT tower design definitions.

The along wind identification for the Av07, presented in Fig.3(a), was discrepant between the OMA tools. OMA SSI-COV had high variability for below and above rated wind speeds' eigen frequencies, resulting in high damping ratios' deviation. The reasons for those behaviors are addressed in Sec.4.3, analyzing a broader variety of samples.

4.3. OMA-SSI - Sensibility Analysis on Full-Scale Data

The whole month of November 2015 (11/2015) was analyzed (1440 samples of 30-minutes average and 50Hz) in order to verify features affecting OMA SSI-COV performance, specially in highly damped responses.

The along wind damping ratio presented a wide variability at almost all wind speeds, with no clear relation to nacelle yaw or TI factor, as shown in Fig.4. Same can be said to the acceleration RMS, wave direction and atmospheric instability. This suggest that OMA SSI-COV poor performance in highly damped modes is driven by numerical uncertainty or incorrect automated

parameters' tuning.

(a) Nacelle Mean Yaw (°)

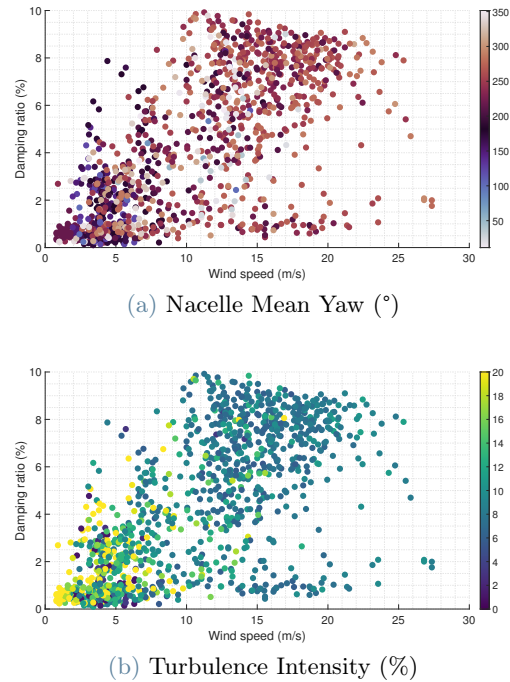(b) Turbulence Intensity (%)

Figure 4: Along Wind Damping Sensibility Analysis for Av07 (11/2015) - OMA SSI-COV.

Figure 5, diversely, allows the visualization of a correlation between the scatter cross wind damping at low wind speeds and both the mean nacelle yaw (100°-150°) and TI (above 18%).
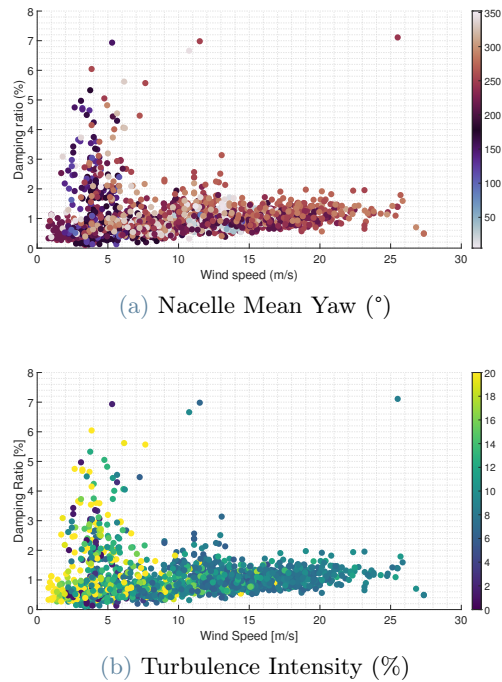

(a) Nacelle Mean Yaw (°)

(b) Turbulence Intensity (%)

Figure 5: Cross Wind Damping Sensibility Analysis for Av07 (11/2015) - OMA SSI-COV.

5.   Conclusions

The thesis work concluded that

- The OMA techniques were able to identify the along wind and cross wind distinct eigen frequencies' and damping ratios' behaviors, for both simulated and full-scale data. In the second case, the white noise excitation assumption is not fully respected due to inevitable non-stationary meteorological conditions in a real wind park and yet the OMA tools showed to be robust.

Afterward, the OMA tools had their performance analyzed in terms of mean and deviation in the modal damping ratio's identification.

- The along wind modal damping ratios were significantly higher than for the cross wind in all methods applied. This highlights the aerodynamic contribution to the overall OWT tower's damping.
- OMA SSI-COV presented a better match with MLD reference than OMA Sing for the cross wind motion, assumed as lightly damped. Besides that, the OMA SSI-COV performance is worsened when higher TI factors are revealed.
- A significant limitation was seen for the more complex OMA SSI-COV along wind identification. The meteorological and controller conditions did not appear to have a clear relation. This suggested that OMA SSI-COV has numerical limitations on the identification of highly damped modes (above 3%), which were not observed for the OMA Sing samples.

6.   Acknowledgments

Data Availability Statement

References

[1] Rune Brincker and Carlos Ventura. *Introduction to operational modal analysis*. John Wiley & Sons, 2015.

[2] E. Cheynet. Operational modal analysis with automated ssi-cov algorithm, 2020.

[3] E. Cheynet. Operational modal analysis with single sensor, 2021.

[4] Muammer Ozbek, Fanzhong Meng, and Daniel Jean Rixen. Challenges in testing and monitoring the in-operation vibration characteristics of wind turbines. *Mechanical Systems and Signal Processing*, 41:649–666, 2013.

[5] Wojciech Popko, Matthias L Huhn, Amy Robertson, Jason Jonkman, Fabian Wendt, Kolja Müller, Matthias Kretschmer, Fabian Vorpahl, Torbjørn Ruud Hagen, Christos Galinos, et al. Verification of a numerical model of the offshore wind turbine from the alpha ventus wind farm within oc5 phase iii. In *International Conference on Offshore Mechanics and Arctic Engineering*, volume 51319, page V010T09A056. American Society of Mechanical Engineers, 2018.